Journal of Geophysical Research: Solid Earth

Supporting Information for

Three-Dimensional Basin Depth Map of the Northern Los Angeles Basins from Gravity and Seismic Measurements

V. Villa[1], Y. Li[1], R. W. Clayton[1], and P. Persaud[2]

[1]California Institute of Technology, Pasadena, CA, 91125. [2]Louisiana State University, Baton Rouge, LA, 70803.

Contents of this file

Introduction

The supporting information includes 5 out of the 10 lines mentioned in the manuscript. Lines SG3, SG4, SB3, SB5, and SB6 are shown here. Each figure shows the receiver function profile and the time-to-basement interpretations of Ghose et al. (2022) and Wang et al. (2021). The Bouguer gravity and residual Bouguer gravity values are shown. The shear-wave velocity model from Li et al. (2022) used to calculate the basement depth is shown and the basement depth is shown. For reference to each of the line's locations, a map with relevant fault locations is included.

Table S1 outlines the boreholes used to constrain the depth of the basement. The units of depth are in meters. The unique well number, or API, is provided for detailed information on the borehole's data.

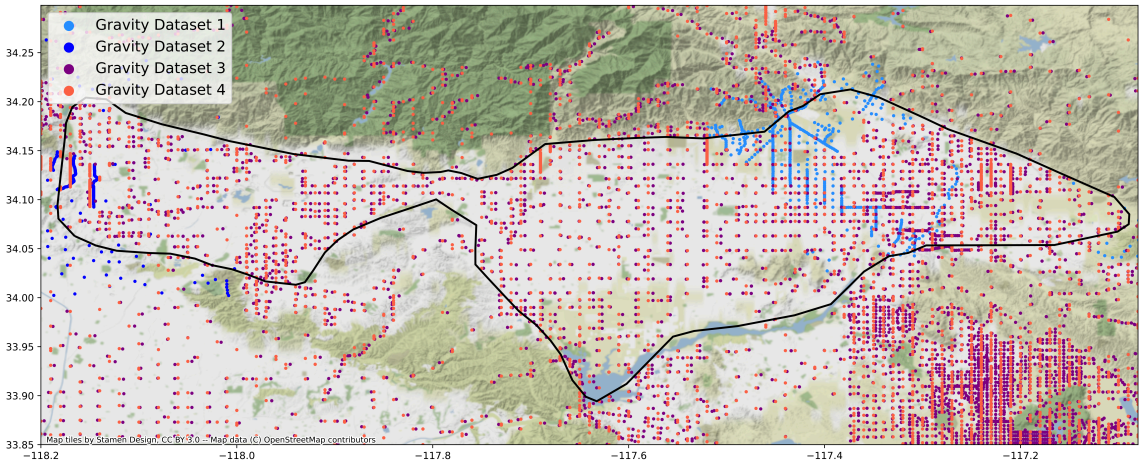

Figure S1. Gravity data set stations were obtained from (*PACES*, 2012). Individual data set stations are colored in different colors.

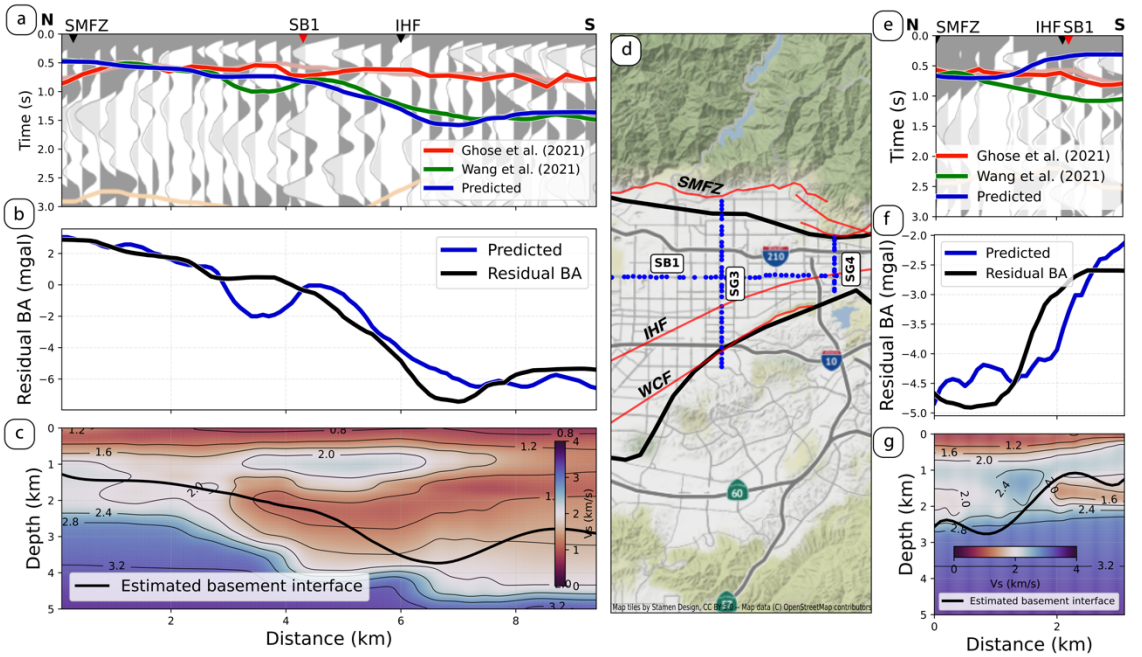

Figure S2. a) Profile along SG3 showing the time-to-basement from two RF studies and the predicted time-to-basement from this study. RF background from Ghose et al. (2022) is from a single event and the faint yellow line is an intra-crustal layer. b) Residual and predicted Bouguer anomaly is shown with black and blue lines, respectively. c) Shear wave velocity cross-section from Li et al. (2022) and the estimated basement surface determined by converting the blue line in a) to depth. d) Map showing the nodal stations of the SG3 and SG4 lines as blue dots. SB1 stations are included for reference. Maroon lines are fault locations. IHF, Indian Hill Fault; SMFZ; Sierra Madre Fault Zone; WCF, Walnut Creek Fault. e) Profile along SG4 showing the time-to-basement from two RF studies and the predicted time-to-basement from this study. RF background from Ghose et al. (2021) is from a single event. f) Residual and predicted Bouguer anomaly is shown with black and blue lines, respectively. g) Shear wave velocity cross-section from Li et al.

(2022) and the estimated basement surface determined by converting the blue line in e) to depth.

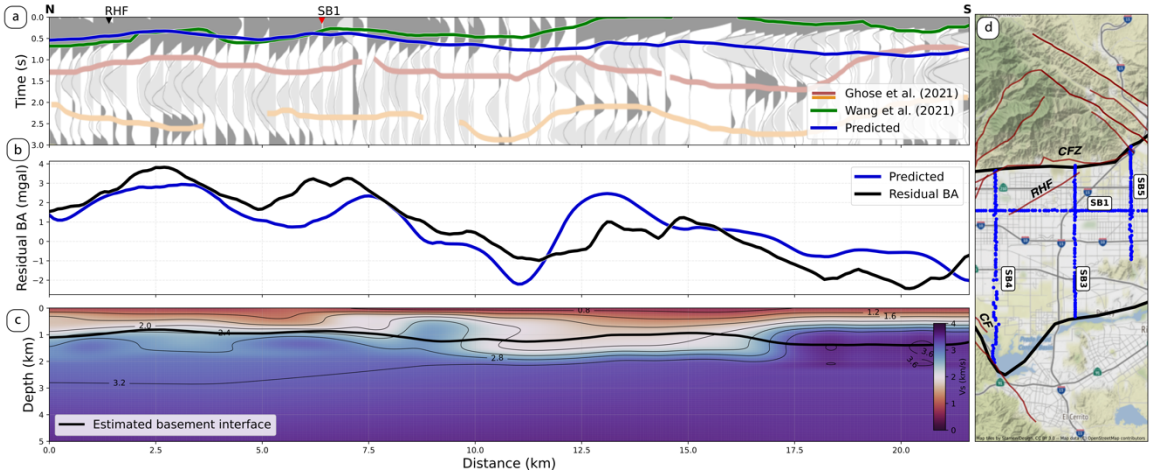

Figure S3. a) Profile along SB3 showing the time-to-basement from two RF studies and the predicted time-to-basement from this study. RF background from Ghose et al. (2022) is from a single event and the faint yellow line is an intra-crustal layer. b) Residual and predicted Bouguer anomaly is shown with black and blue lines, respectively. c) Shear wave velocity cross-section from Li et al. (2022) and the estimated basement surface determined by converting the blue line in a) to depth. d) Map showing the nodal stations of the SB3 line as blue dots. SB1, SB4, and SB5 stations are included for reference. Maroon lines are fault locations. CF, Chino Fault; CFZ, Cucamonga Fault Zone; RHF, Red Hill Fault.

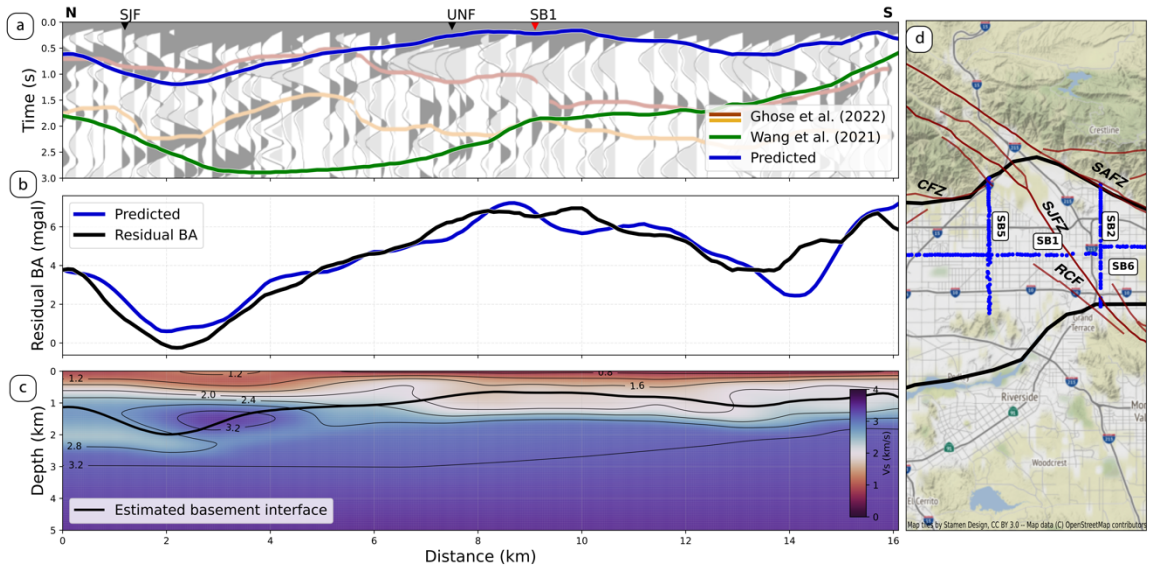

Figure S4. a) Profile along SB5 showing the time-to-basement from two RF studies and the predicted time-to-basement from this study. RF background from Ghose et al. (2022) is from a single event and the faint yellow line is an intra-crustal layer. b) Residual and predicted Bouguer anomaly is shown with black and blue lines, respectively. c) Shear

wave velocity cross-section from Li et al. (2022) and the estimated basement surface determined by converting the blue line in a) to depth. d) Map showing the nodal stations of the SB5 line as blue dots. SB1, SB2, and SB6 stations are included for reference. Maroon lines are fault locations. CFZ, Cucamonga Fault Zone; RCF, Rialto Colton Fault; SAFZ, San Andreas Fault Zone; SJFZ, San Jacinto Fault Zone.

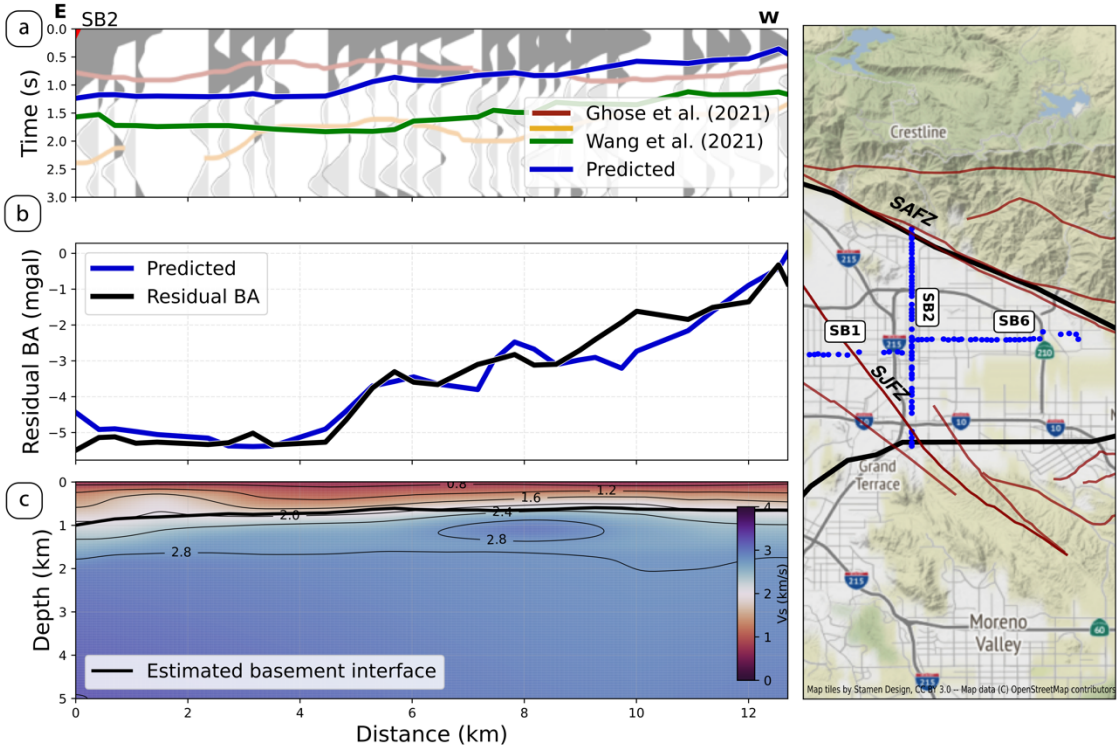

Figure S5. a) Profile along SB6 showing the time-to-basement from two RF studies and the predicted time-to-basement from this study. RF background from Ghose et al. (2022) is from a single event and the faint yellow line is an intra-crustal layer. b) Residual and predicted Bouguer anomaly is shown with black and blue lines, respectively. c) Shear wave velocity cross-section from Li et al. (2022) and the estimated basement surface determined by converting the blue line in a) to depth. d) Map showing the nodal stations of the SB6 line as blue dots. SB1 and SB2 stations are included for reference. Maroon lines are fault locations. SAFZ, San Andreas Fault Zone; SJFZ, San Jacinto Fault Zone.

	Name	API	Well Depth (m)	Modeled Depth (m)
1	Southern Pacific	0403706338	723	1600
2	South San Gabriel	0403705501	1402	1800
3	Harmon	0403705790	1790	1850
4	Cordova	0403720575	1798	1800
5	Puente One	0403706114	1812	2200
6	Puente Nine	0403706115	1800	1800

7	Consolidated	4003705962	2170	2900
8	McGinnis	4003706092	2301	2050
9	Rosemead	0403720665	2590	1950
10	El Monte	0403721403	2616	3350
11	Ferris	0403705964	3715	3050
12	Dana	0407100024	542	750
13	Donald B. Lamond	0407100083	725	1000
14*	C-68	Buwalda (1940)	228	228
15*	C-10s	Buwalda (1940)	243	243
16*	C-17	Buwalda (1940)	251	251
17*	C-127	Buwalda (1940)	350	350

Table S1. Boreholes were used in the study to calibrate and validate the model. The numbering indicates the location in figure 7. Wells 1-13 were obtained through the CalGEM website and are searchable through this API number. Wells 14-17 were obtained from Buwalda's (1940) report.

* Wells used to calculate depth for the Raymond Basin.

References

Buwalda, J. P. (1940). *Geology of the Raymond Basin* (pp. 1–131). California Institute of Technology. http://doi.org/10.22002/D1.20258

Ghose, R., Persaud, P., Wang, X., & Clayton, R. W. (2022). *High-frequency receiver function profiles reveal sedimentary basin structure beneath the northern Los Angeles area* [In-preparation].

Li, Y., Villa, V., Clayton, R., & Persaud, P. (2022). *Shear Wave Velocities in the San Gabriel and San Bernardino Basins, California* (world). https://doi.org/10.1002/essoar.10512118.1

PACES. (2012). Pan-American Center for Earth and Environmental Studies. http://gis.utep.edu/paces/PACES%20Gravity%20Magnetics.htm

Wang, X., Zhan, Z., Zhong, M., Persaud, P., & Clayton, R. W. (2021). Urban Basin Structure Imaging Based on Dense Arrays and Bayesian Array-Based Coherent Receiver Functions. *Journal of Geophysical Research: Solid Earth*, *126*(9). https://doi.org/10.1029/2021JB022279